Materials Letters 94 (2013) 165–168

Contents lists available at SciVerse ScienceDirect

Materials Letters

journal homepage: www.elsevier.com/locate/matlet

Interfacial structure of *a*-plane ZnO grown on *r*-plane sapphire by pulsed laser deposition

Chun-Yen Peng*, Wei-Lin Wang, Yen-Teng Ho, Jr-Sheng Tian, Li Chang*

Department of Materials Science and Engineering, National Chiao Tung University, Hsinchu, Taiwan

ARTICLE INFO

Article history:
Received 17 October 2012
Accepted 1 December 2012
Available online 8 December 2012

Keywords:
Nonpolar ZnO
Epitaxial growth
Interfaces
HRTEM
RSM

ABSTRACT

In this study, interfacial structure of *a*-ZnO with misfit accommodation on *r*-sapphire at low and high growth temperatures (LT and HT) by pulsed laser deposition is presented. Along $[1\bar{1}00]_{ZnO}$ of large lattice mismatch of ZnO with sapphire, TEM examinations show that *a*-type misfit dislocations are spaced 1.3–2.2 nm on HT-ZnO/sapphire interface, whereas dislocation pairs in spacing of 2.8–3.5 nm are observed for LT-ZnO/sapphire. For smaller lattice mismatch along the ZnO *c*-axis direction, reciprocal space maps of $(11\bar{2}\bar{2})_{ZnO}$ and $(30\bar{3}0)_{sapphire}$ reflections show that HT-ZnO is nearly fully strained without much relaxation and has a highly coherent interface with sapphire, in contrast with partial relaxation in LT-ZnO.

© 2012 Elsevier B.V. All rights reserved.

1. Introduction

As a wide direct bandgap wurtzite semiconductor, zinc oxide (ZnO) is an attractive material for potential applications in optoelectronic devices [1–4]. Recently, growth of nonpolar epitaxial films has attracted a lot of interest due to the lack of the red-shift caused by the quantum-confined Stark effect [5,6]. Because the spontaneous polarization of ZnO is nearly two times of GaN (-0.057 to $0.05\ C/m^2$ versus -0.029 to $-0.022\ C/m^2$) [7,8], ZnO films without polarity along the growth direction are important for light emitting applications.

Sapphire is a commonly used substrate for growth of epitaxial thin films. Nonpolar $(11\bar{2}0)$ *a*-ZnO epitaxial films grown on $(10\bar{1}\bar{2})$ *r*-sapphire substrates have been achieved by domain matching epitaxy methods [9] using pulsed laser deposition (PLD) [10], sputtering [11], plasma-assisted molecular beam epitaxy [12–13], and metal–organic chemical vapor deposition [14]. From domain matching epitaxial relationships of $[000\bar{1}]_{ZnO}//[10\bar{1}1]_{sapphire}$ and $[1\bar{1}00]_{ZnO}//[\bar{1}2\bar{1}0]_{sapphire}$, anisotropic stresses resulted from anisotropic lattice and thermal mismatches may have significant effects on its crystallinity [15–17]. It has been shown that the misfit is relaxed by regularly spaced misfit dislocations along the large lattice mismatch direction of $[1\bar{1}00]_{ZnO}$, whereas misfit dislocations are hardly seen along the ZnO *c*-direction due to its small lattice misfit [12,17–19]. In addition, the densities of threading dislocations (TDs) and stacking faults are often observed in $10^8-10^{10}\ cm^{-2}$ and 10^4–$10^5\ cm^{-1}$, respectively [18–20].

It is known that growth temperature plays an important role on crystallinities and optical properties [11,21–22]. However, the variation of strains and misfit accommodations with different growth temperatures has been rarely studied. In our previous study, we have shown that the transition of the film growth mode may occur at 600 °C for *a*-ZnO grown on *r*-sapphire [22]. In this paper, we show that misfit accommodations along in-plane directions are indeed varied with growth temperature from the evidence of transmission electron microscopy (TEM) and x-ray reciprocal space mapping (RSM).

2. Experiments

ZnO films were grown on $8\times8\ mm^2$ *r*-sapphire wafers at 10 mTorr oxygen partial pressure in a Pascal laser-MBE system at 450 °C (LT-ZnO) and 750 °C (HT-ZnO). The KrF excimer laser irradiation with the energy density of about 1–3 J/cm^2 and the repetition rate of 2 Hz was used to ablate a sintered ZnO target. Sapphire substrates were ultrasonically cleaned in acetone before loading into the vacuum chamber. Before PLD growth, 850 °C thermal cleaning of the substrate in vacuum at about 10^{-6} Torr was done for 30 min.

A Philips Tecnai 20 TEM operated at 200 kV was employed to investigate microstructures of ZnO on sapphire. The preparation of cross-sectional TEM (XTEM) specimens was carried out using mechanical grinding process and Ar^+ ion milling at 3.5–4.0 kV. The RSM experiments were performed in a PANalytical X'Pert Pro

* Corresponding authors. Tel.: +886 3 5731615; fax: +886 3 5724727.
E-mail addresses: cypeng.mse94g@nctu.edu.tw (C.-Y. Peng), lichang@cc.nctu.edu.tw (L. Chang).

0167-577X/$ - see front matter © 2012 Elsevier B.V. All rights reserved.
http://dx.doi.org/10.1016/j.matlet.2012.12.003

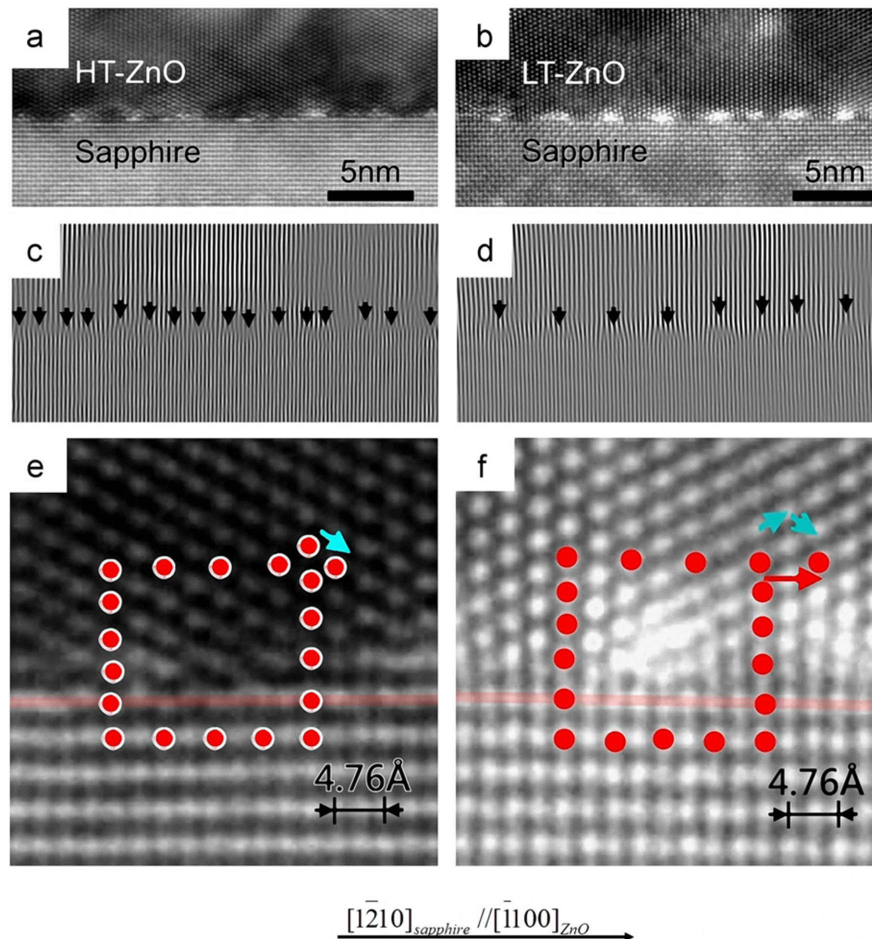

Fig. 1. HRTEM micrographs of (a) HT-ZnO/sapphire and (b) LT-ZnO/sapphire interface viewed along $[0001]_{ZnO}$. (c,d) Fourier-filtered images of (a,b) using $(1\bar{1}00)_{ZnO}$ and $(\bar{1}2\bar{1}0)_{sapphire}$ reflections. (e,f) Enlarged images of (a,b), points and arrows are Burgers circuits and vectors respectively.

(MRD) system employing a Ge (220) monochromator and Ge (220) channel cut analyzer.

3. Results and discussion

High-resolution XTEM micrographs of 180 nm HT-ZnO and LT-ZnO on *r*-sapphire viewed along $[0001]_{ZnO}$ are shown in Fig. 1(a) and (b), respectively. Also, the Fourier-filtered images in Fig. 1(a) and (b) using $(1\bar{1}00)_{ZnO}$ and $(\bar{1}2\bar{1}0)_{sapphire}$ reflections are shown in Fig. 1(c) and (d), respectively. From $(1\bar{1}00)_{ZnO}$ and $(\bar{1}2\bar{1}0)_{sapphire}$ lattice fringes, the extra-half planes of misfit dislocations can be clearly observed. For the HT-ZnO/sapphire interface in Fig. 1(c), the extra-half planes have a spacing of 1.3–2.2 nm as often seen in literature [12,18,19,23], whereas 2.8–3.5 nm spacing between adjacent misfit dislocations is observed for the LT-ZnO/sapphire interface in Fig. 1(d). In the in-plane direction of $[1\bar{1}00]_{ZnO}$, the translation period of ZnO and sapphire lattices are 5.63 Å and 4.76 Å, respectively. Due to large lattice mismatch of 18.3%, introduction of misfit dislocations with edge component of Burgers vector (**b**) in $[1\bar{1}00]_{ZnO}$ is required. In our previously study, the difference in initial growth behavior between HT- and LT-ZnO had been observed [24]. It may closely correlate with different misfit accommodation mechanisms.

As the Burgers circuit failure in Fig. 1(e) gives $b=1/3\langle\bar{2}110\rangle_{ZnO}$ in *a*-type, misfit dislocations in the interface between HT-ZnO and sapphire can have a component (0.28 nm) of $1/2\langle\bar{1}100\rangle_{ZnO}$ in the interface. For the LT-ZnO/sapphire interface in Fig. 1(f), the MDs have $b=\langle\bar{1}100\rangle_{ZnO}$. Even with 18.3% misfit it is only possible for *a*-ZnO to grow on *r*-sapphire with domain matching epitaxy, where the misfit can be accommodated by matching of $5\times[\bar{1}100]_{ZnO}$ with $6\times\frac{1}{3}[1\bar{2}10]_{sapphire}$ (domain misfit$=\frac{5\times5.63-6\times4.76}{6\times4.76}=-1.4\%$) or $6\times[\bar{1}100]_{ZnO}$ with $7\times\frac{1}{3}[1\bar{2}10]_{sapphire}$ (domain misfit$=\frac{6\times5.63-7\times4.76}{7\times4.76}=1.4\%$). Since the translation periods of ZnO and sapphire lattices in this direction are 5.63 and 4.76 Å, respectively, the spacing of MDs of $b=[\bar{1}100]_{ZnO}$ is ~2.8–3.4 nm. However, those dislocations with $b=[\bar{1}100]_{ZnO}$ are unstable due to b^2 energy criterion where $b=|b|$. Therefore, it may decompose to two *a*-type dislocations as $[\bar{1}100]=1/3[\bar{2}110]+1/3[\bar{1}2\bar{1}0]$ in a more stable configuration [25].

Because the horizontal component along the interface is $1/2[1\bar{1}00]_{ZnO}$, the spacing of *a*-type misfit dislocations is reduced to ~1.4–1.7 nm. Moreover, a $[1\bar{1}00]$ misfit dislocation has two extra-half planes [25], whereas only one extra-half plane is present with an *a*-type misfit dislocation. For LT-ZnO, most of the MDs shown in Fig. 1(d) appear either in pairs of *a*-type dislocations or $[1\bar{1}00]$ MDs as seen in Fig. 1(f) with two extra-half planes. In contrast, the MDs observed in Fig. 1(c) for HT-ZnO are pure *a*-type MDs as the Fourier-filtered image in Fig. 1(e) shows only one half plane associated with each MD.

Fig. 2 shows high-resolution XTEM images of 180 nm HT-ZnO/sapphire and LT-ZnO/sapphire viewed along $[1\bar{1}00]_{ZnO}$. The corresponding Fourier-filtered images using $(0002)_{ZnO}$ and $(10\bar{1}4)_{sapphire}$ reflections are shown in Fig. 2(c) and (d). Different

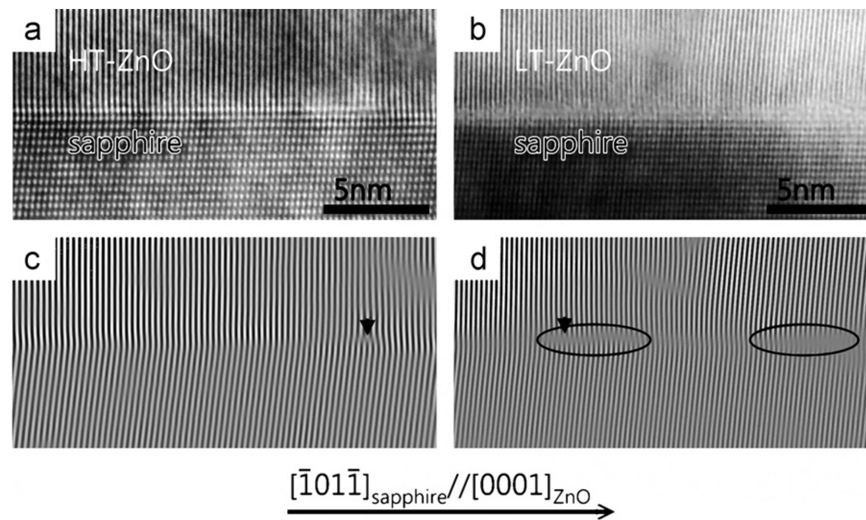

Fig. 2. HRTEM micrographs of (a) HT-ZnO/sapphire and (b) LT-ZnO/sapphire interface viewed along $[\bar{1}100]_{ZnO}$. (c,d) Fourier-filtered images of (a,b) using $(0002)_{ZnO}$ and $(10\bar{1}4)_{sapphire}$ reflections. MDs and non-perfect regions are indicated by arrows and circles respectively.

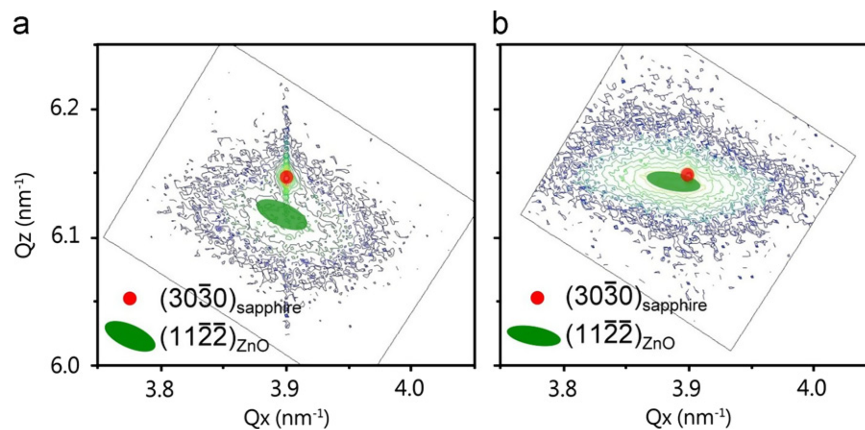

Fig. 3. Reciprocal space maps of (a) HT-ZnO and (b) LT-ZnO films showing $(11\bar{2}\bar{2})_{ZnO}$ and $(30\bar{3}0)_{sapphire}$ reflections.

from those observed in Fig. 1, MDs are rarely observed in this view due to small lattice misfit in ZnO *c*-direction similar to the previous reports [11,16–18]. For HT-ZnO, however, an extra-half plane marked by arrow shown in Fig. 2(c) may be occasionally observed in the TEM examinations across a wide range of a few micrometers. In contrast, more extra-half planes can be found along the LT-ZnO/sapphire interface in this direction, implying that more strain relaxation occurs.

Fig. 3 shows $(11\bar{2}\bar{2})_{ZnO}$ and $(30\bar{3}0)_{sapphire}$ RSMs for HT- and LT-ZnO. For HT-ZnO, Fig. 3(a) shows nearly vertically aligned $(11\bar{2}\bar{2})_{ZnO}$ and $(30\bar{3}0)_{sapphire}$ reflections indicating that HT-ZnO is almost fully strained with sapphire in this direction, while 0.39% residual misfit ($\xi_c=([0001]_{ZnO}-1/3[\bar{1}01\bar{1}]_{Sapphire})/1/3[\bar{1}01\bar{1}]_{Sapphire}$) is present for LT-ZnO as shown in Fig. 3(b). It is known that misfit strain can be relaxed by introducing MDs which have an edge component along the interface. More amount of MDs observed in LT-ZnO/sapphire are helpful to relax the misfit between $[0001]_{ZnO}$ and $[\bar{1}01\bar{1}]_{Sapphire}$, while rare MDs for HT-ZnO in this direction are resulted from nearly fully strained lattice.

4. Conclusions

In summary, distinctly different misfit accommodations for HT-ZnO on *r*-sapphire from that for LT-ZnO are observed by the HRTEM observations in cross section. MD pairs are spaced with 2.8–3.5 nm at the interface for LT-ZnO along $[\bar{1}100]_{ZnO}$, whereas HT-ZnO exhibits individual *a*-type MDs spaced with 1.3–2.2 nm. Furthermore, there are a few MDs along the ZnO *c*-direction for LT-ZnO, but MDs are rarely observed for HT-ZnO.

Acknowledgments

This research was partially supported by the National Science Council, Taiwan, ROC. under Grant no. NSC98-2221-E-009-042-MY3.

References

[1] Aoki T, Hatanaka Y, Look DC. Appl Phys Lett 2000;76:3257.
[2] Guo XL, Choi JH, Tabata H, Kawai T. Jpn J Appl Phys 2001;40:L177.
[3] Tsukazaki A, Kubota M, Ohtomo A, Onuma T, Ohtani K, Ohno H, et al. Jpn J Appl Phys 2005;44:L643.
[4] Ryu Y, Lee TS, Lubguban JA, White HW, Kim BJ, Park YS, et al. Appl Phys Lett 2006;88:241108.
[5] Makino T, Ohtomo A, Chia CH, Segawa Y, Koinuma H, Kawasaki M. Physica E 2004;21:671.
[6] Makino T, Segawa Y, Kawasaki M, Koinuma H. Semicond Sci Technol 2005;20:S78.
[7] Bernardini F, Fiorentini V, Vanderbilt D. Phys Rev B 1997;56:R10024.
[8] Lähnemann J, Brandt O, Jahn U, Pfüller C, Roder C, Dogan P, et al. Phys Rev B 2012;86:081302(R).
[9] Narayan J, Larson BC. J Appl Phys 2003;93:278.
[10] Srikant V, Sergo V, Clarke DR. J Am Ceram Soc 1995;78:1931.

[11] Kim YJ, Kim YT, Yang HK, Park JC, Han JI, Lee YE, et al. J Vac Sci Technol A 1997;15:1103.
[12] Han SK, Hong SK, Lee JW, Lee JY, Song JH, Nam YS, et al. J Cryst Growth 2007;309:121.
[13] Yamauchi S, Handa H, Nagayama A, Hariu T. Thin Solid Films 1999;345:12.
[14] Liu Y, Gorla CR, Liang S, Emanetoglu N, Lu Y, Shen H, et al. J Electron Mater 2000;29:69.
[15] Saraf G, Lu Y, Siegrist T. Appl Phys Lett 2008;93:041903.
[16] Pant P, Budai JD, Narayan J. Acta Mater 2010;58:1097.
[17] Chauveau JM, Vennéguès P, Laügt M, Deparis C, Zuniga-Perez J, Morhain C. J Appl Phys 2008;104:073535.
[18] Lee JW, Han SK, Hong SK, Lee JY, Yao T. J Cryst Growth 2008;310:4102.
[19] Lee JW, Han SK, Hong SK, Lee JY. Appl Surf Sci 2010;256:1849.
[20] Han SK, Kim JH, Hong SK, Song JH, Song JH, Lee JW, et al. J Cryst Growth 2010;312:2196.
[21] Pant P, Budai JD, Aggarwal R, Narayan RJ, Narayan J. Acta Mater 2009;57:4426.
[22] Peng CY, Tian JS, Wang WL, Ho YT, Chuang SC, Chu YH, et al. J Vac Sci Technol A 2011;29:03A110.
[23] Zhou H, Chisholm MF, Pant P, Chang HJ, Gazquez J, Pennycook SJ, et al. Appl Phys Lett 2010;97:121914.
[24] Peng CY, Tian JS, Wang WL, Ho YT, Chang L doi:10.1016/j.apsusc2012.11.044, In press .
[25] Osipiyan Yu A, Smirnova IS. Phys Status Solidi 1968;30:19.